RSC Advances

ROYAL SOCIETY OF CHEMISTRY

www.rsc.org/advances

An ideal nanostructure of polymer/$BaTiO_3$ dielectric materials with high reliability for breakdown strength: Isolated and uniformly dispersed $BaTiO_3$ nanoparticles by thick polymer shells

Kenichi Hayashida,*[a] Yoriko Matsuoka[b] and Yasuhiro Takatani[b]

[a] *Materials and Processing Dept. II, Toyota Central R&D Labs., Inc., Nagakute, Aichi 480-1192, Japan. E-mail: e1440@mosk.tytlabs.co.jp*

[b]*Materials Analysis and Evaluation Dept., Toyota Central R&D Labs., Inc., Nagakute, Aichi 480-1192, Japan*

Poly(methyl methacrylate)s (PMMAs) with various chain lengths were grafted on barium titanate (BT) particles using surface-initiated polymerization. The obtained core-shell particles were blended with additional PMMA to yield nanocomposites where the BT particles could not approach each other by the PMMA shells (PMMA-BT). It was confirmed that the BT particles were uniformly dispersed in PMMA-BT by SEM observation. Reliability for the dielectric properties of PMMA-BT was evaluated under an alternating current electric field at 50 Hz using 16 specimens, and compared to that of conventional nanocomposites prepared by blending PMMA with the unmodified BT nanoparticles. The homogeneous distribution of the BT particles for PMMA-BT had no great influence on the reliability for complex relative permittivity while much improved the reliability for dielectric breakdown strength E_{DB}. The superior reliability for the E_{DB} of PMMA-BT would result from the absence of percolation of the BT particles in the PMMA-BT system. This finding demonstrates the nanostructure where the BT particles are isolated and uniformly dispersed by polymer shells is ideal for high E_{DB} reliability.

Introduction

Dielectric materials are popularly used to store electrical energy as capacitors [1]. Among the

dielectric materials, polymer materials have the advantages of high flexibility, lightness, and processability. The highly flexible polymer materials are also promising for other applications such as actuators and sensors [2-6]. However, the very low dielectric constant ε_r' of the polymer materials (ε_r' = 2–3) strongly impedes the potential applications. Because of the high ε_r' of ceramic materials (ε_r' > 100), therefore, polymer/ceramics composite materials have been much developed over the last few decades. Barium titanate (BT), one of ferroelectric metal oxides, has been most widely used for enhancement in ε_r' [7-21]. However, it is well-known that the incorporation of the BT particles usually brings not only reduction in dielectric breakdown strength E_{DB} but also considerably uneven E_{DB} of the obtained composite materials; a defective product with extremely low E_{DB} appears with a given probability. The low reliability for E_{DB} is a serious problem to industrial products.

The extremely low E_{DB} of the polymer/BT composites would be mainly due to the formation of a three-dimensional network of the BT particles in the polymer matrix, that is, percolation of the BT particles. The probability of the percolation is highly increased by aggregation of the BT particles and inhomogeneous distribution of the aggregates in the polymer matrix [22]. Surface modification of the BT particles with silane coupling reagents is an effective method to reduce the aggregation of the BT particles. Besides the silane coupling agents, small organic molecules such as phosphonic acids have been used for surface modification of the BT particles [8,11]. When the strong interaction between the BT particles is suppressed and the compatibility with the polymer matrix is improved by the surface modifications, the BT particles, in turn, should be randomly packed in the polymer matrix. According to the percolation theory with a random packing, the probability of the percolation is quite low when the volume fraction of the BT particle Φ_{BT} is below a critical value, known as a percolation threshold. Therefore, the appropriate surface modification that produces the random packing of the BT particles can be effective to prevent the percolation of the BT particles in the composite with low Φ_{BT}. However, in the composite with Φ_{BT} above the percolation threshold, the surface modification cannot prevent the percolation of the BT particle, resulting in the

extremely low E_{DB} of the polymer/BT composite. When spherical BT particles are randomly packed in a polymer matrix, the Φ_{BT} at the percolation threshold is estimated to be about 0.30 [23,24].

The percolation of the BT particles can be perfectly forbidden if each BT particle is isolated and uniformly dispersed in the polymer matrix. A solution to realize the ideal nanostructure for the polymer/BT composite materials would be polymer grafting on the BT particle. Thick polymer shells over 10 nm formed by polymer grafting on the BT particles can keep the distance between the BT particles as long and uniform as possible. Jiang and coworkers have prepared BT nanoparticles grafted with poly(methyl methacrylate) (PMMA) by surface-initiated atom transfer radical polymerization (SI-ATRP) techniques [14]. Whereas the dielectric properties of the PMMA-grafted BT nanocomposites have been investigated in the study, the E_{DB} of the nanocomposites has not been reported. On the other hand, we have also established a SI-ATRP technique of synthesizing high molecular weight polymethacrylates densely grafted on nanoparticles using an originally designed ATRP initiator, *p*-(bromomethyl)benzyl 2-bromoisobutylate (BBnBiB) [25]. Using our SI-ATRP technique, poly(cyclohexyl methacrylate) (PCHMA) was densely grafted on multiwalled carbon nanotubes (CNTs), and the dielectric properties of the PCHMA-grafted CNT nanocomposites have been comprehensively studied [26-28].

In this paper, we demonstrate that polymer/BT nanocomposites where the BT nanoparticles are isolated and uniformly dispersed by thick polymer shells, exhibit high reliability for E_{DB}. A series of PMMA-grafted BT nanoparticles with various polymer thicknesses (> 10 nm) (BT@PMMA) was synthesized using our SI-ATRP technique, and blended with additional PMMA matrix to yield the polymer/BT nanocomposites (PMMA-BT). The reliability for the complex relative permittivity ε_r of PMMA-BT was investigated under an alternating current (AC) electric field at 50 Hz using 16 specimens, and compared to that of conventional nanocomposites prepared by blending PMMA with the unmodified BT nanoparticles (PMMA/BT). Subsequently, using the identical specimens, the E_{DB}'s of the two series of composites were measured at the same frequency of 50 Hz and

evaluated by Weibull analysis. To our knowledge, this is the first report that the reliability for both the ε_r and the E_{DB} of polymer/BT composite materials were systematically characterized using the identical specimens at the same frequency. Furthermore, we observed the distribution of the BT particles in the PMMA matrix using a combination of a cross section polisher (CP) [29] and a scanning electron microscope (SEM). A relationship between the distribution of the BT nanoparticles and the dielectric properties of the nanocomposites was also revealed.

Experimental

Sample Preparation

BT particles with an average diameter of 100 nm were obtained from Wako Pure Chemical Industries (Japan). The density of the BT particle was determined to be 5.73 g cm^{-3} using an ultrapycnometer. Procedures for modification of the BT particles were as follows:

Amine-modification of the BT particles: *N*-[3-(Trimethoxysilyl)propyl]aniline (450 μl, 1.9 mmol) and hexylamine (90 μl, 0.68 mmol) were added to the BT particles (18 g) homogeneously dispersed in acetonitrile (AN) (90 ml) containing small amount of water (0.9 ml). The dispersion was sonicated and kept at 50 ºC for 3 h. The amine-modified BT particles (BT-NHPh) were purified by 3 cycles of filtration and redispersion in AN.

Immobilization of ATRP initiators on the BT particles: *p*-(Bromomethyl)benzyl 2-bromoisobutylate (0.96 g, 2.7 mmol) and 1,8-bis(dimethylamino)naphthalene (0.26 g, 1.2 mmol) were added to BT-NHPh dispersed in AN (20 ml). The mixture was sonicated and kept at 40 ºC for 6 h. The initiator-modified BT particles (BT-Br) were purified by 3 cycles of filtration and redispersion in AN.

Surface-initiated polymerization from the BT particles: *N,N*-Dimethylacetamide (30-50 ml) was added to BT-Br (2.9–5.8 g) and CuBr (28.6 mg, 200 μmol) in a vacuum. After sonication of the mixture, 2,2'-bipyridyl (62.4 mg, 400 μmol) in methyl methacrylate (30-10 ml) was added, and the

dispersion was kept at 60 ºC for 6 h. The resultant core-shell particles (BT@PMMA) were precipitated in methanol and purified by 2 cycles of dissolving in benzene and centrifugation.

PMMA-BT nanocomposites were prepared by blending BT@PMMA with an additional PMMA matrix. First, BT@PMMA and the PMMA matrix were added in benzene and homogeneously dispersed by sonication. The dispersion was quickly frozen by liquid nitrogen, and then freeze-dried under vacuum. Similarly, PMMA/BT nanocomposites were also prepared. Thus-obtained two types of nanocomposites were molded into disklike specimens with a diameter of 15 mm and a thickness of ~0.2 mm by compression of at 130 ºC. For electrical measurements, 16 specimens were prepared for each sample, and two gold electrodes with a diameter of 9 mm were deposited on the top and bottom of the specimens.

Measurements

The BT contents in the BT@PMMA, PMMA/BT and PMMA-BT were determined by thermogravimetry. The sample taken in a platinum pan was heated with a thermobalance (Rigaku, Thermo Plus TG 8120) from room temperature to 600 ºC at a rate of 10 ºC min^{-1} under an air flow (200 ml/min). The cross-section of the specimen that had been flattened by CP was observed using an SEM (Hitachi, S-4300) operated at an accelerating voltage of 2 kV. SEM images of the BT@PMMA core-shell particles were obtained at an accelerating voltage of 5 kV. DC resistance of the specimen was measured using a megohmmeter (Hioki, SM-8220) under a nitrogen atmosphere, and the value was recorded after 10 minute from voltage application of 500 V. Complex permittivity at 50 Hz was obtained at 20 V using an LCR meter (Agilent, E4980A), and the frequency dependence in the range of 10^{-2}–10^{6} Hz was measured at 2 V using an impedance analyzer (Solartron, 126096W). Dielectric breakdown test was performed using the short-time method. The specimen was placed in oil at 23 ºC, and AC voltage with 50 Hz was applied to the specimen at a rate of 2 kV min^{-1}.

Results and Discussion

ATRP-initiator modified BT particles (BT-Br) was synthesized as shown in Fig. 1, where the BT particles with an average diameter of 100 nm was used. In the first step, amine-functionalized BT particle (BT-NHPh) was prepared using a silane coupling reagent containing an aromatic amine group. In the second step, BT-NHPh was reacted with BBnBiB, and the ATRP-initiator moiety was introduced on the BT surface (BT-Br). Methyl methacrylate was polymerized from BT-Br, and PMMA chains were grafted on the BT particles (BT@PMMA). Three kinds of core-shell particles with various PMMA chain lengths (BT@$PMMA_L$, BT@$PMMA_M$, and BT@$PMMA_S$) were synthesized as listed in Table 1. The core-shell structures are clearly observed in high resolution SEM images of the BT@PMMA particles in Fig. 2. The thicknesses of the PMMA shells for BT@$PMMA_M$ and BT@$PMMA_L$ are about 20 and 40 nm, respectively, and consistent with the theoretical values calculated from the average diameter of the BT particle and Φ_{BT} (Table 1). The BT@PMMA particles were blended with additional PMMA matrix (that is, ungrafted PMMA) to yield a series of the PMMA-BT nanocomposites (Table 1). The ungrafted PMMA was added to fill space between the BT@PMMA particles, and the volume fraction of the ungrafted PMMA in PMMA-BT was fixed to be around 0.33. Conventional nanocomposites (PMMA/BT) were also prepared by blending the pristine BT particles with PMMA, and designed to have the same Φ_{BT} as PMMA-BT. The two types of nanocomposite samples were molded by hot pressing. The dispersivity of the BT nanoparticles in the molded specimens for these nanocomposites was observed by SEM. In this SEM observation, the surfaces of the specimens had been flattened with argon ion beam using a cross section polisher (CP) [29]. Fig. 3 shows SEM images of the two types of nanocomposites with Φ_{BT} = 0.21. For PMMA/BT, the BT nanoparticles are inhomogeneously dispersed although compatibility between PMMA and BT particles is known to be high [30,31]. This inhomogeneity is essentially inevitable for polymer/BT composites prepared by blending even if the random distribution of the BT particles is achieved by high compatibility between the polymer matrix and the BT particles. In contrast, the dispersivity of the BT particles is surprisingly well for PMMA-BT. In the PMMA-BT system, the BT particles are forced to be isolated and

uniformly dispersed by the thick PMMA shells. We suggest polymer-grafting should be the best method of producing the perfectly homogeneous dispersion of BT particles in a polymer matrix.

For electrical measurements, 16 specimens were carefully prepared for each sample, and gold electrodes were deposited on the specimens by sputter coating. First, the complex relative permittivity ε_r for the two types of nanocomposites was measured under an AC electric filed at 50 Hz. The dielectric constant ε_r' and dielectric loss factor ε_r" values of all the specimens are plotted in Fig. 4a. In this study, in order to evaluate the reliability for ε_r, coefficient of variation (CV) for ε_r' and ε_r" was compared between PMMA/BT and PMMA-BT as shown in Fig. 4b and c. There is no great difference in CV for ε_r' and ε_r" between PMMA/BT and PMMA-BT. This is because the ε_r of the specimen is the average values in a whole one. Therefore, the inhomogeneous distribution of the BT particles for PMMA/BT has no serious influence on the CV values for ε_r. Fig. 5 shows the mean values for the ε_r's of the 16 specimens as a function of Φ_{BT}. PMMA-BT has smaller ε_r' than PMMA/BT, which implies that the ε_r' of a polymer/BT composite is more decreased as the BT particles are more homogeneously dispersed in the polymer matrix. The phenomenon has already been reported, and a detailed explanation was discussed in the reference [28]. Moreover, Wang and Tan have also demonstrated that a composite with agglomerated particles exhibited slightly higher ε_r' than that with well-dispersed particles using a simulation method [32]. In addition, it is known that the ε_r' of a polymer/BT composite can be described by Lichteneker's logarithmic mixing rule as follows [7,10,12,28]:

$$\varepsilon_r' = \varepsilon_{rm}' \cdot (\varepsilon_{rBT}'/\varepsilon_{rm}')^{\Phi BT}, \quad (1)$$

where ε_{rm}' and ε_{rBT}' are the ε_r's of the polymer matrix and the BT particle. Notice that the ε_{rBT}' is an apparent ε_r' of the BT particle in the polymer matrix, and not the ε_r' of the corresponding bulk BT. Generally, the apparent ε_{rBT}' is much smaller than the ε_r' of the corresponding bulk BT, because the BT particles cannot form a continuous phase in the polymer/BT composite system; the interface between the BT particles drastically reduces the apparent ε_{rBT}'. Also, the apparent ε_{rBT}' is affected by the dispersivity of the BT particles in the matrix as well as the form of the BT particle [28]. The

apparent $\varepsilon_r'_{BT}$ is known to be 80-210 according to some literatures [11,12,28]. The fitting curves of Lichteneker's logarithmic mixing rule for PMMA/BT and PMMA-BT are drawn in Fig. 5 in broken and solid lines, respectively. For PMMA/BT, the theoretical curve that well fits to the experimental result gives the apparent $\varepsilon_r'_{BT}$ of 130 at 50 Hz, which is similar to the reported values. On the other hand, the apparent $\varepsilon_r'_{BT}$ of 72 is obtained for PMMA-BT, suggesting the better dispersion of the BT particles.

Frequency f dependence for the ε_r of the two types of nanocomposites is shown in Fig. 6. In this measurement, the specimen that has ε_r' and ε_r'' values close to the mean ε_r' and ε_r'' for the 16 specimens was used for each sample. Broad dielectric relaxation peaks related to the PMMA matrix are observed at around 50 Hz in all the spectra for ε_r''. In addition, another dielectric relaxation peaks can be recognized in the lower f range for PMMA/BT with Φ_{BT} = 0.21 and 0.30. Considering that the corresponding relaxation peak is absent for PMMA-BT, the relaxation peak would result from charge transfer between the BT particles. The charge transfer is expected to have an influence on direct current volume resistivity (ρ_{DC}) of PMMA/BT. Fig. 7 shows the ρ_{DC} of the two types of nanocomposites. PMMA/BT has lower ρ_{DC} than PMMA-BT.

After the measurements for ε_r, dielectric breakdown (DB) strength E_{DB} was measured at 50 Hz using the identical specimens. A relationship between the ε_r' and E_{DB} values of the specimens is plotted in Fig. 8. For each nanocomposite series, there is a tendency that the E_{DB} values of the specimens are low as the ε_r' values are high. This trade-off relationship also appears in a set of the 16 specimens for each sample. In addition, the results for E_{DB} were characterized using Weibull analysis [33]. Unlike ε_r, E_{DB} is determined by the weakest local structure of a whole specimen, and the DB phenomenon can be statistically explained using weakest-link theory introduced by Weibull. According to the weakest-link theory, cumulative probability P for DB is expressed by the following equation:

$$P = 1–\exp[–(E_{DB}/\alpha)^{\beta}], \quad (2)$$

where α is a scale parameter that represents the E_{DB} at the P of 63.2% (known as the characteristic E_{DB}) and β is a shape parameter. Then, eqn (2) is deformed as,

$$\log[-\ln(1-P)] = \beta \log E_{DB} - \beta \log \alpha, \quad (3)$$

Therefore, if DB events are caused by a single mechanism, the data lie on a straight line in a plot of $\log[-\ln(1-P)]$ against $\log E_{DB}$ called a Weibull plot. Fig. 9 shows Weibull plots for the E_{DB} of the two types of nanocomposites, where the P of the E_{DB} value is obtained by the median rank approximation. All the 16 points for each sample are on a straight line except for PMMA/BT with $\Phi_{BT} = 0.30$. For PMMA/BT with $\Phi_{BT} = 0.30$, 4 points have the extremely lower E_{DB} values than the other 12 points lying on a straight line. This could be attributed to percolation of the BT particles occurring in the specimens. According to the percolation theory with a random packing of spherical particles, the percolation threshold is calculated to be about 0.30 [23,24]. Therefore, it is considered that PMMA/BT with $\Phi_{BT} = 0.30$ had an unignorable probability of the percolation, resulting in the appearance of the 4 specimens with the extremely low E_{DB}. In this DB test, the specimens with an electrode area of only 0.64 cm^2 were used. If the electrode area had been larger, the appearance probability of the specimen with the extremely low E_{DB} would have been much greater owing to the percolation of the BT particles. In contrast, PMMA-BT exhibits the superior reliability for E_{DB} because no percolation occurred in the PMMA-BT system where the BT particles were isolated and uniformly dispersed by thick polymer shells. This finding demonstrates the nanostructure is ideal for high E_{DB} reliability.

In summary, we synthesized barium titanate (BT) nanoparticles grafted with poly(methyl methacrylate)s (PMMAs) with various chain lengths and prepared nanocomposites by blending the core-shell particles with additional PMMA (PMMA-BT). It is confirmed that the BT particles were uniformly dispersed in PMMA-BT by SEM observation. Reliability for the dielectric properties of PMMA-BT was measured under an AC electric field at 50 Hz using 16 specimens, and compared to that of conventional nanocomposites prepared by blending PMMA with the unmodified BT nanoparticles. The homogeneous distribution of the BT particles for PMMA-BT had no great

influence on the reliability for complex relative permittivity ε_r while much improved the reliability for dielectric breakdown strength E_{DB} at higher BT loading. This is because unlike ε_r, E_{DB} is determined by the weakest local structure of a whole specimen. The high reliability for the E_{DB} of PMMA-BT would result from the absence of percolation of the BT particles in the PMMA system.

References

1 W. J. Sarjeant, J. Zirnheld, F. W. MacDougall, J. S. Bowers, N. Clark, I. W. Clelland, R. A. Price, M. Hudis, I. Kohlberg, G. McDuff, I. McNab, S. G. Parler Jr. and J. Prymak, in *Handbook of Low and High Dielectric Constant Materials and Their Applications*, ed. H. S. Nalwa, Academic Press, London, 1999, vol. 2, ch. 9, 423-491.

2 P. Brochu and Q. Pei, *Macromol. Rapid Commun.*, 2010, **31**, 10-36.

3 S. Risse, B. Kussmaul, H. Krüger and G. Kofod, *Adv. Funct. Mater.*, 2011, **21**, 4589-4594.

4 B. Kussmaul, S. Risse, G. Kofod, R. Wache, M. Wegener, D. N. McCarthy, H. Krüger and R. Gerhard, *RSC Adv.*, 2012, **2**, 9029-9035.

5 S. C. B. Mannfleld, B. C.-K. Tee, R. M. Stoltenberg, C. V. H.-H. Chen, S. Barman, B. V. O. Muir, A. N. Sokolov, C. Reese and Z. Bao, *Nature Mater.*, 2010, **9**, 859-864.

6 D. J. Cohen, D. Mitra, K. Peterson and M. M. Maharbiz, *Nano Lett.*, 2012, **12**, 1821-1825.

7 S.-D. Cho, S.-Y. Lee, J.-G. Hyun and K.-W. Paik, *J. Mater. Sci. Mater. Electron.*, 2005, **16**, 77-84.

8 P. Kim, S. C. Jones, P. J. Hotchkiss, J. N. Haddock, B. Kippelen, S. R. Marder and J. W. Perry, *Adv. Mater.*, 2007, **19**, 1001-1005.

9 J. Lu and C. P. Wong. *IEEE Trans. Dielectr. Insul.*, 2008, **15**, 1322-1328.

10 K.-W. Jang and K.-W. Paik, *J. Appl. Polym. Sci.*, 2008, **110**, 798-807.

11 P. Kim, N. M. Doss, J. P. Tillotson, P. J. Hotchkiss, M.-J. Pan, S. R. Marder, J. Li, J. P. Calame and J. W. Perry, *ACS Nano*, 2009, **3**, 2581-2592.

12 Y. Kobayashi, A. Kurosawa, D. Nagao and M. Konno, *Polym. Eng. Sci.*, 2009, **49**, 1069-1075.

13 H. M. Jung, J.-H. Kang, S. Y. Yang, J. C. Won and Y. S. Kim, *Chem. Mater.*, 2010, **22**, 450-456.

14 L. Xie, X. Huang, C. Wu and P. Jiang, *J. Mater. Chem.*, 2011, **21**, 5897-5906.

15 M.-F. Lin, V. K. Thakur, E. J. Tan and P. S. Lee, *RSC Adv.*, 2011, **1**, 576-578.

16 S. Siddabattuni, T. P. Shuman and F. Dogan, *Mater. Sci. Eng. B*, 2011, **176**, 1422-1429.

17 Z.-M. Dang, J.-K. Yuan, J.-W. Zha, T. Zhou, S.-T. Li and G.-H. Hu, *Prog. Mater. Sci.*, 2012, **57**, 660-723.

18 Y. Song, Y. Shen, H. Liu, Y. Lin, M. Li and C.-W. Nan, *J. Mater. Chem.*, 2012, **22**, 16491-16498.

19 L. Xie, X. Huang, Y. Huang, K. Yang and P. Jiang, *ACS Appl Mater Interfaces*, 2013, **5**, 1747-1756.

20 K. Yang, X. Huang, Y. Huang, L. Xie and P. Jiang, *Chem. Mater.*, 2013, **25**, 2327-2338.

21 B.-H. Fan, J.-W. Zha, D.-R. Wang, J. Zhao, Z.-F. Zhang and Z.-M. Dang, *Compos. Sci., Technol.*, 2013, **80**, 66-72.

22 S. F. Wang and A. A. Ogale, *Compos. Sci., Technol.*, 1993, **46**, 93-103.

23 G. E. Pike and C. H. Seager, *Rhys. Rev. B*, 1974, **10**, 1421-1434.

24 C. D. Lorenz and R. M. Ziff, *J. Chem. Phys.*, 2001, **114**, 3659-3661.

25 K. Hayashida, H. Tanaka and O. Watanabe, *Polymer*, 2009, **50**, 6228-6234.

26 K. Hayashida and H. Tanaka, *Adv. Funct. Mater.*, 2012, **22**, 2338-2344.

27 K. Hayashida, *RSC Adv.*, 2013, **3**, 221-227.

28 K. Hayashida and Y. Matsuoka, *Carbon*, 2013, **60**, 506-513.

29 N. Erdman, R. Campbeli and S. Asahina, *Microsc. Today*, 2006, **14**, 22-25.

30 D.-W. Kim, D.-H. Lee, B.-K. Kim, H.-J. Je and J.-G. Park, *Macromol. Rapid Commun.*, 2006, **27**, 1821-1825.

31 J. Lott, C. Xia, L. Kosnosky, C. Weder and J. Shan, *Adv. Mater.*, 2008, **20**, 3649-3653.

32 Y. U. Wang and D. Q. Tan, *J. Appl. Phys.*, 2011, **109**, 104102.

33 W. Weibull, *J. Appl. Mech.*, 1951, **18**, 293-302.

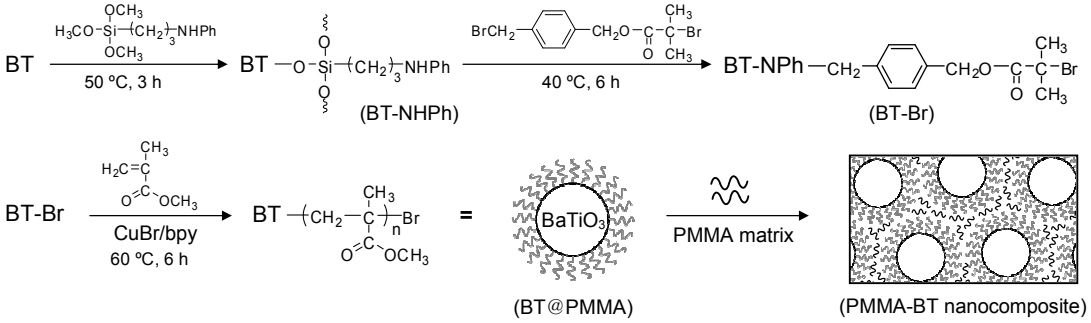

Fig. 1 Preparation procedure of PMMA-BT nanocomposites.

Table 1 Characteristics of BT@PMMA core-shell particles and two types of nanocomposites.

Sample	Φ_{BT} [a]	Φ_{PMMA}		PMMA shell thickness [nm] [b]
		grafted	ungrafted	
BT@PMMA$_L$	0.163	0.837	–	43.2
BT@PMMA$_M$	0.325	0.675	–	23.6
BT@PMMA$_S$	0.446	0.554	–	16.0
PMMA-BT	0.111	0.570	0.319	43.2
	0.213	0.442	0.345	23.6
	0.301	0.374	0.325	16.0
PMMA/BT	0.107	–	0.893	–
	0.214	–	0.786	–
	0.293	–	0.707	–

[a] Calculated using a bulk density of 5.73 g cm^{-3} for the BT and of 1.18 g cm^{-3} for the organic components. [b] Calculated from the average diameter of the BT particle and Φ_{BT}.

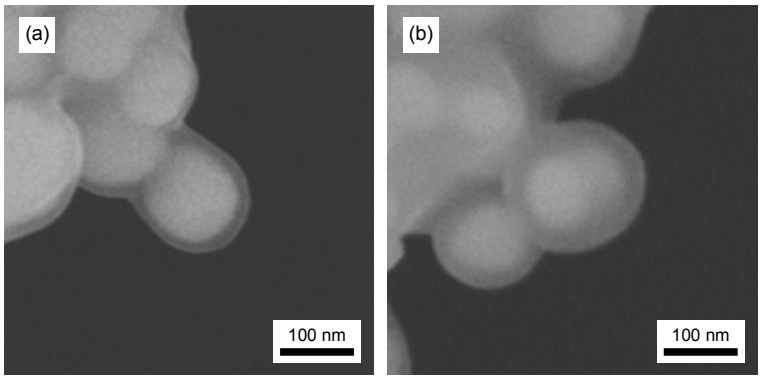

Fig 2 High resolution SEM images of (a) BT@$PMMA_M$ and (b) BT@$PMMA_L$ particles.

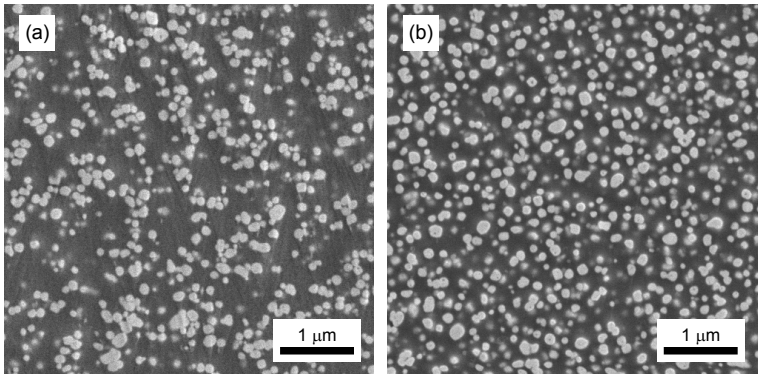

Fig 3 SEM images of (a) PMMA/BT and (b) PMMA-BT nanocomposites with $\Phi_{BT} = 0.21$.

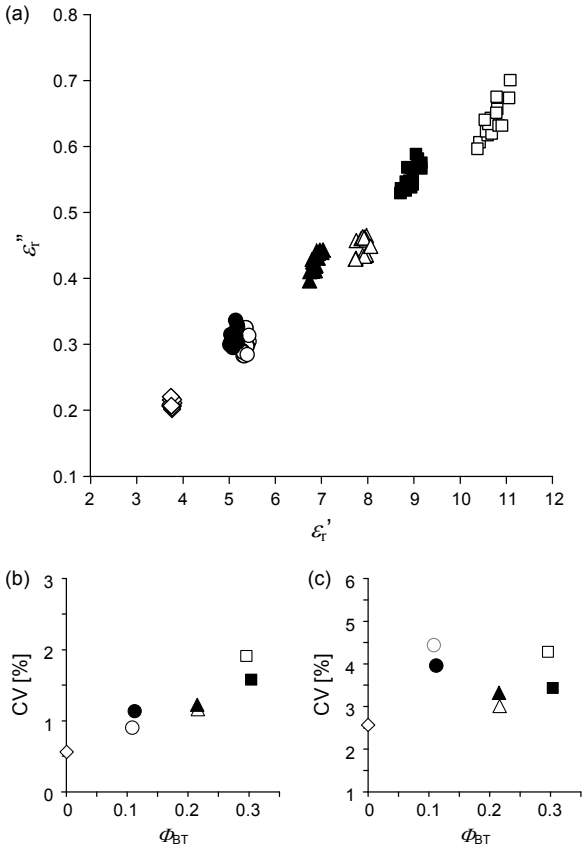

Fig 4 (a) Distribution of ε_r' and ε_r" of PMMA (diamonds) and two types of nanocomposites with Φ_{BT} = 0.11 (circles), Φ_{BT} = 0.21 (triangles), and Φ_{BT} = 0.30 (squares), and coefficient of variation for (b) ε_r' or (c) ε_r". Open symbols, PMMA/BT; filled symbols, PMMA-BT. 16 specimens were measured for each sample at 50 Hz.

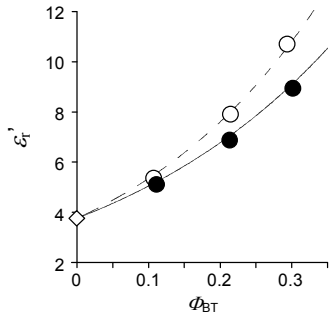

Fig 5 ε_r' of PMMA (diamond) and two types of nanocomposites (circles) at 50 Hz as a function of Φ_{BT}. Open symbols, PMMA/BT; filled symbols, PMMA-BT. The plots are fitted by Lichtenecker's logarithmic mixing rule and the curves are shown in broken and solid lines for PMMA/BT and PMMA-BT, respectively.

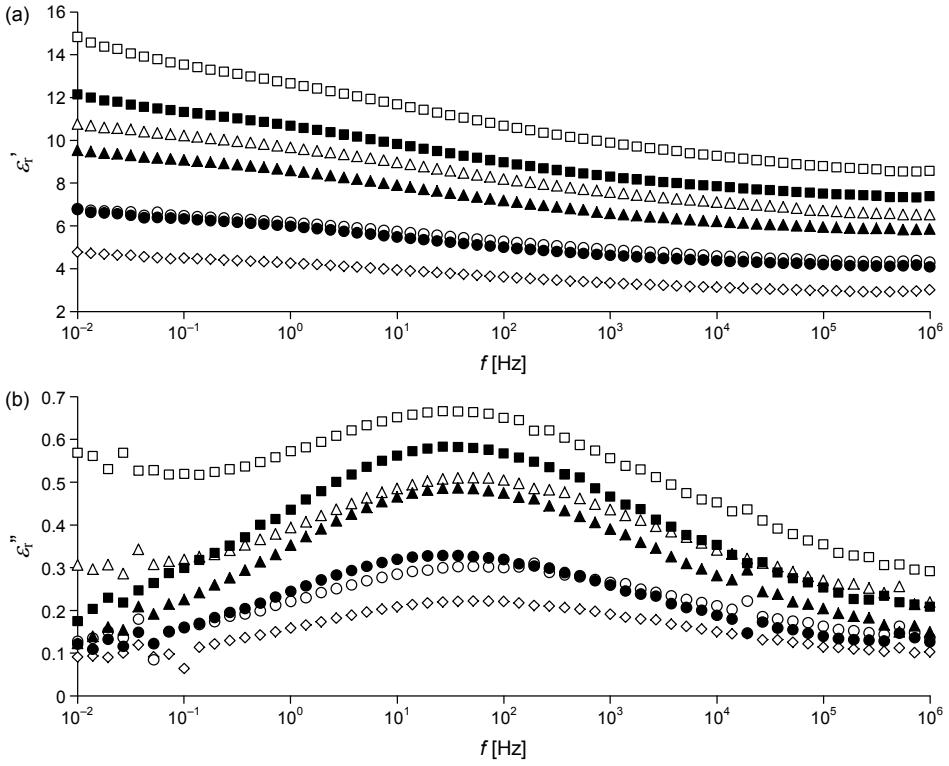

Fig 6 Frequency f dependence of (a) ε_r' and (b) ε_r" of PMMA (diamonds) and two types of nanocomposites with Φ_{BT} = 0.11 (circles), Φ_{BT} = 0.21 (triangles), and Φ_{BT} = 0.30 (squares). Open symbols, PMMA/BT; filled symbols, PMMA-BT.

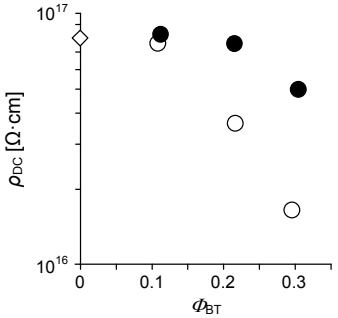

Fig 7 DC volume resistivity ρ_{DC} of PMMA (diamond) and two types of nanocomposites (circles) as a function of Φ_{BT}. Open symbols, PMMA/BT; filled symbols, PMMA-BT.

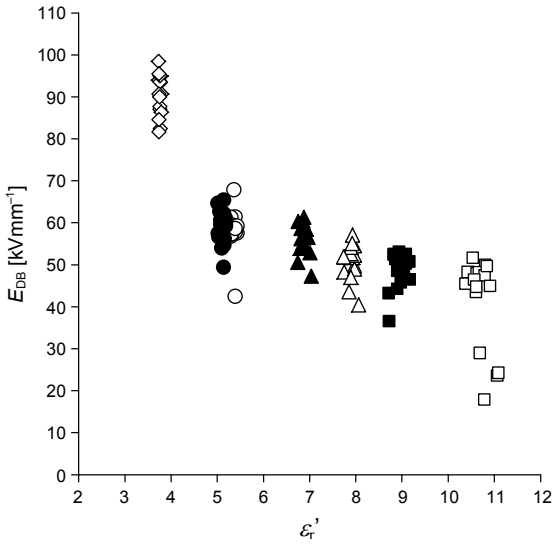

Fig 8 Distribution of ε_r" and E_{DB} of PMMA (diamonds) and two types of nanocomposites with Φ_{BT} = 0.11 (circles), Φ_{BT} = 0.21 (triangles), and Φ_{BT} = 0.30 (squares). Open symbols, PMMA/BT; filled symbols, PMMA-BT. 16 specimens were measured for each sample at 50 Hz.

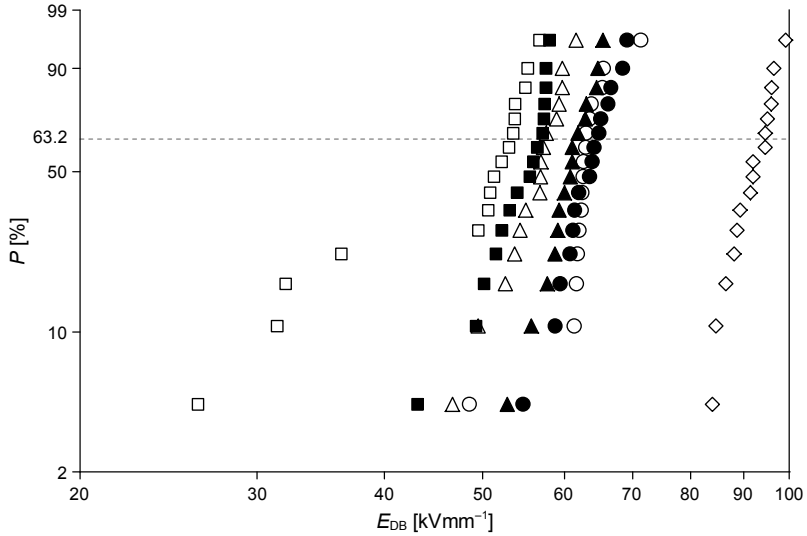

Fig 9 Weibull plots of E_{DB} at 50 Hz for PMMA (diamonds) and two types of nanocomposites with Φ_{BT} = 0.11 (circles), Φ_{BT} = 0.21 (triangles), and Φ_{BT} = 0.30 (squares). Open symbols, PMMA/BT; filled symbols, PMMA-BT.